THE ASTROPHYSICAL JOURNAL, 448:271–280, 1995 July 20

VARIATION OF GRAVITATIONAL DELAY IN PULSAR TIMING OBSERVATION DUE TO PROPER MOTION OF FOREGROUND STARS AND MEASUREMENT OF STELLAR MASS

KOUJI OHNISHI
Kansai Advanced Research Center, Communications Research Laboratory, Kobe 651-24, Japan; ohnishi@crl.go.jp
MIZUHIKO HOSOKAWA
Communications Research Laboratory, Koganei, Tokyo 184, Japan; hosokawa@crl.go.jp
TOSHIO FUKUSHIMA
National Astronomical Observatory, Mitaka, Tokyo 181, Japan; toshio@spacetime.mtk.nao.ac.jp
AND
MINE TAKEUTI
Astronomical Institute, Tohoku University, Aoba-ku, Sendai 980-77, Japan
Received 1994 October 3; accepted 1995 February 3

ABSTRACT

We propose the inclusion of a new correction term, the gravitational time delay effect caused by a star between the observer and the pulsar, in the analysis of pulsar timing observation. This effect appears in the form of $\ln(1 + t^2)$, where the amplitude connects directly to the mass of the star. When the residuals of the time of arrival have a positive hump, it is worthwhile to reanalyze the data by including this correction term in the existing models. The analysis of this effect will not only help to stabilize the pulsar time but also provide a new way to determine the mass of a star directly. When the mass of a star is 0.2 $M_\odot$, the observation accuracy is 200 ns, and the observation period is 10 yr, the possibility of detecting this effect is of the order of one-hundredth.

Subject headings: astrometry — dark matter — pulsars: general — relativity — stars: fundamental parameters

1. INTRODUCTION

The mass of a star is one of the most fundamental quantities in astrophysics. However, its measurement is very difficult, especially in the case of a single star and massive compact halo objects (MACHOs), a kind of dark matter candidates in the Galactic halo (Aubourg et al. 1993; Alcock et al. 1993; Udalski et al. 1993). Since the general relativistic effects depend on the mass of the gravitating matter, these effects can be used for the measurement of stellar mass. A well-known example is the microlensing effect, the amplification of the luminosity of a star by the gravitational lensing of the foreground star. The duration of the luminosity enhancement depends on the mass, the distance and the proper motion of the lensing star. So if we know the distance and the proper motion by a separate method, the mass will be evaluated (Paczyński 1986). Recently, we proposed another method to measure the stellar mass by use of the gravitational lensing (Hosokawa et al. 1993). In this case, the mass and the distance of the lensing star can be determined simultaneously by observing the parallactic variation of gravitational deflection of the light from the lensed source. In this paper, we present yet another method to measure the stellar mass. This time we consider the detection of the variation of the gravitational time delay of pulses from pulsar caused by foreground stars.

In order to detect the gravitational time delay, we have to know the original timing of pulse emission very precisely and have to observe the delayed signals very accurately. Among pulsars, millisecond pulsars are known to have a long-term stability in the pulse period and have been proved to be one of the most stable "clocks" of all known natural phenomena. The observational accuracy of the time of arrival (TOA) of pulse from millisecond pulsars has presently reached the level of a few hundred nanoseconds (Kaspi, Taylor, & Ryba 1994). Since the TOAs are measured in the proper time of the moving observer, they must be related to that of the pulsar. In the existing models of the TOA data analysis (Taylor & Weisberg 1989, for example), the variation of the TOAs has been considered to be caused by (1) the change of the behavior of the pulsar itself and (2) the dynamical motions of the observer and the pulsar.

As for the variation of the TOAs, the gravitational time delay caused by the Sun, known as the Shapiro delay, and the delay caused by the pulsar's companion(s) in the case of binary pulsars, have been taken into account (Shapiro 1964; Backer & Hellings 1986; Ryba & Taylor 1991). On the other hand, the gravitational time delay caused by a third body, such as a star between the observer and the pulsar, has been ignored. This is because (1) this effect is not separable from the clock offset unless the relative configuration of the observer, the star, and the pulsar changes, and (2) even if the configuration changes, this time delay will vary linearly with time approximately and therefore will be absorbed into the dynamical effects. The variation of this effect would be, however, observable in some cases.

In § 2, we will describe the theory of this effect and will estimate its magnitude. In § 3, the separability of this effect from other causes of the TOA variation and the possibility of mass measurement by this method will be considered. Some related topics are discussed, and the summary is presented in § 4.

2. THEORY

Consider that an observer O, a foreground star S, and a pulsar P are well aligned, and the separation between the

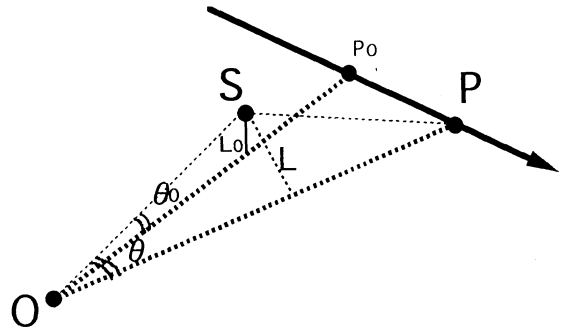

FIG. 1.—Configuration of the observer O, the pulsar P, and the star S. The separation between the pulsar and the star seen from the observer ∠SOP, denoted by θ, changes with time due to the proper motion of the star relative to the pulsar. The length between S and the pulse path PO is L. At the epoch of the closest approach $t = t_0$, the pulsar is located at P_0. The minimum of θ and L are θ_0 and L_0, those when $t = t_0$, respectively.

pulsar and the star seen from the observer changes with time due to the proper motions of them. A pulse from P is delayed by the gravitational field of S and arrives at O. Here we describe the system so that the star is at rest and the pulsar moves with constant velocity (see Fig. 1). Then the amount of the gravitational time delay is approximately expressed as

$$\Delta t(t) = \text{constant} - (1+\gamma)\frac{GM_S}{c^3}\ln\left|1+\left(\frac{t-t_0}{t_d}\right)^2\right|, \quad (1)$$

where γ is a parameterized post-Newtonian (PPN) parameter, G is the Newton's universal constant of gravitation, M_S is the mass of the star, and c is the speed of light in vacuum, t_0 is the epoch of the closest approach,

$$t_d \equiv \frac{\theta_0}{\mu} \quad (2)$$

is the characteristic timescale of this effect, θ_0 is the minimum of $\theta \equiv \angle$POS, and μ is the proper motion of the pulsar relative

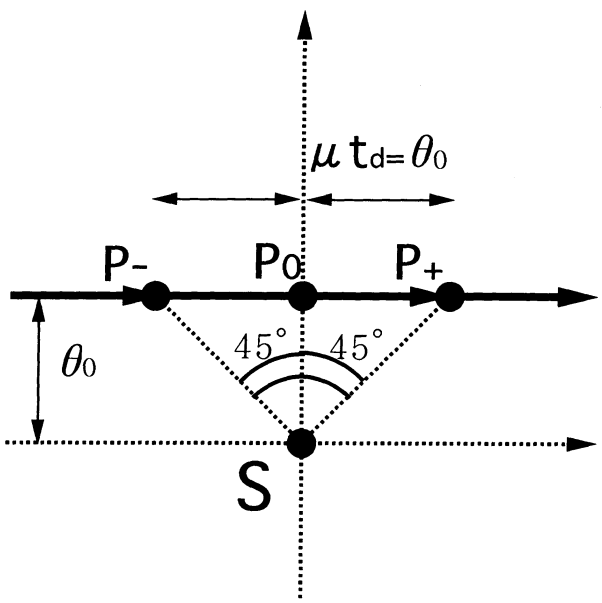

FIG. 2.—Apparent motion of the pulsar P relative to the gravitating star S. The point P_0 denotes the closest position of the pulsar P at the time $t = t_0$. When $t = t_0 \pm t_d$, the pulsar is located in $P_\pm$, respectively. The angle $\angle P_\pm P_0 S$ is 45°.

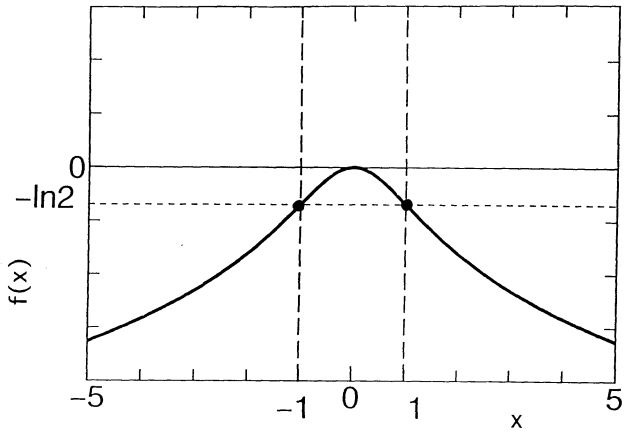

FIG. 3.—Characteristic function $f(x) = -\ln(1+x^2)$. The curve has only one maximum at $x = 0$ and has two inflection points at $x = \pm 1$ where the values are both $-\ln 2 \approx -0.693$. These points correspond to P_0 when $t = t_0$ and $P_\pm$ when $t = t_0 \pm t_d$ in Fig. 2, respectively.

to the star. Equation (1) is an approximation under the condition that both of θ and ∠OPS are sufficiently small. See Appendix A for the detailed derivation. Figure 2 illustrates the apparent motion of P relative to S, where P_0 denotes the closest position when $t = t_0$ and $P_\pm$ are the positions when $t = t_0 \pm t_d$.

First we remark that, in equation (1), the magnitude of the delay is in proportion to the mass of the star directly. It has no explicit dependence on the distances to the star or the pulsar, on the impact parameter, or on the closest separation angle between the star and the pulsar. This is the most important point which differs from the microlensing or the parallactic variation of gravitational lensing where the mass is coupled with the distance.

Next, the time variation of the delay depends not on the least-impact parameter itself but on its ratio to that of the displacement of the foreground star during the observation period. The time dependency of the delay is characterized by a function

$$f(x) = -\ln(1+x^2), \quad (3)$$

which has the following features: (1) it is symmetric with the argument x, (2) it has the only one maximum 0 at $x = 0$, (3) it has two inflection points at $x = \pm 1$ where the values are both $-\ln 2 \approx -0.693$. The variation of $f(x)$ is illustrated in Figure 3. Note that the inflection points correspond to the points $P_\pm$ and $\Delta P_\pm P_0 S$ are rectangular equilateral triangles (see Fig. 2). Namely, the value of the relative displacement during t_d is the same as the length of the least-impact parameter.

Because of features (2) and (3) above, this effect will cause a positive hump in the residuals of TOAs after fitting to the existing models. In that case, the mass of the foreground star will be estimated by the formula

$$M_S = M_\odot \times \frac{H_S}{H_\odot}, \quad (4)$$

where H_S is the height of the hump defined by the difference in time delay between the peak and one of the inflection points (see Fig. 3). The height of the hump for the Sun is evaluated as

$$H_\odot = \ln 2 \times (1+\gamma)\frac{GM_\odot}{c^3} \approx 0.693 \times 9.851\,\mu\text{s} = 6.828\,\mu\text{s}, \quad (5)$$

where we substituted γ by unity as in the case of general theory of relativity. In pulsar timing observation, the typical uncertainty of the TOA is ~ 200 ns. This corresponds to an uncertainty in the mass measurement of as small as 0.03 $M_\odot$. Of course, the smaller the uncertainty in the TOS is, the greater the accuracy of the mass measurement of the star will be.

3. OBSERVABILITY

When the residuals of the TOA have the properties discussed in the preceding section, they might be caused by the gravitational time delay due to foreground stars. In this case, the masses of the stars will be determined from the TOA data analysis by introducing three new parameters M_S, t_0, and t_d. In this section, we will estimate the magnitude of this effect and examine its separability from the other effects considered in the model so far.

In principle, the variation of TOA consists of a periodic part and a systematic trend. The periodic part is caused by the orbital motion of Earth around the solar system barycenter or that of the pulsar around the barycenter of the pulsar system if it has companion(s). The systematic trend has been assumed to be a low-degree polynomial of time, where each degree term represents a different mixture of the intrinsic properties of the pulsar rotation and the dynamical motion of the pulsar relative to the solar system barycenter (see Table 1). In practical TOA data analyses, the degree of the polynomial is set to 2 or 3.

Since the effect introduced in this paper is nonperiodic, it is feasible to separate it from the periodic effects. Note that, although the typical magnitude of the gravitational time delay is relatively large, as of the order of 10 μs, that of the observable effect will be much smaller. This is because the observable quantity is the residual of this delay after the polynomial trend is removed. Let us examine the magnitude of this observable quantity.

First, we will estimate the residuals of this effect after a polynomial fitting. Let us introduce the residual function R per unit gravitating mass for a certain observation period T defined as

$$R = -\ln\left[1 + \left(\frac{t - t_0}{t_d}\right)^2\right] - \sum_{j=0}^{n} c_j\left(\frac{t_d}{T}, \frac{t_0}{T}\right)\left(\frac{t}{T}\right)^j , \quad (6)$$

TABLE 1

CAUSE OF COEFFICIENTS OF POLYNOMIAL REPRESENTING TOA RESIDUALS

Term	Intrinsic	Dynamical
Constant.....	Clock offset	r
Linear.....	v	V_r
Quadratic.....	$\dot{v}$	$\dot{V}_r + r\mu^2$
Cubic	$\ddot{v}$	$\ddot{V}_r + 3r\mu\dot{\mu}$

NOTES.—r is the distance to the pulsar, V_r is the radial velocity of the pulsar, $\dot{V}_r$ is the radial acceleration of the pulsar, $\ddot{V}_r$ is the radial jerk of the pulsar, μ is the proper motion of the pulsar (i.e., $\mu = V_t/r$), and $\dot{\mu}$ is the angular acceleration of the pulsar. Note that the second derivative of the pulse frequency $\ddot{v}$ for most pulsars are small, and this is compatible with the standard radiation theory (Manchester & Taylor 1974), although the observed magnitudes of the cubic term are much larger than the values expected in some cases (see Table 2).

where t_d and t_0 are defined before, and the variable range of t is $|t/T| < 0.5$.

Assume that the motions of the pulsar and the star are both linear and that the deceleration of the pulse period is mainly governed by the magnetic dipole radiation. Then, there are no quadratic and higher terms of dynamical origin because of the linear motion assumption of the pulsar. The cubic and higher trends expected from the radiation theory is so small that they are negligible. Therefore the polynomial is to be second degree.

The coefficients c_j are usually determined from the least-square fitting (see details for Appendix B). Some examples of the expected residual R are shown in Figures 4 and 5. These figures show the amplitude of the residuals as a function of time for some fixed values of t_d/T and t_0/T. Figures 4*a* and 4*b* depict the cases of $t_0 = 0T$ and $t_0 = -0.3T$, while Figures 5*a* and 5*b* show the cases of $t_d = 0.1T$ and $t_d = T$. When the observation period covers the epoch t_0 and T is larger than t_d, the residuals have a large positive hump at the epoch t_0. The smaller t_d/T becomes, the larger the amplitude of the residuals are. When t_0 is the center of the observation period (i.e., $t_0 = 0$), a quartic trend is expected. As t_0 shifts from the center of the observation period, a cubic trend appears gradually.

In order to detect only the effect we proposed, it is sufficient to consider whether the resulting *false* cubic term is detectable, namely, larger than the observation error. However, this is far from determining the three parameters from which we will estimate the mass of a gravitating star. As is clearly seen in the residual cases (3), (5) and (6) of Figure 5, the cubic trend in the residual after a least-square fit taking up to the quadratic term is of the form of P_3, the Legendre's polynomial of third degree, and therefore has only one degree of freedom. Generally speaking, in order to determine the three parameters, we have to consider up to the quintic trend. In the following, we will consider the conditions necessary to detect the effect we proposed and to determine the model parameters, separately.

Let us introduce angular coordinates (θ_x, θ_y) on the celestial sphere such that the star seems to be fixed, the origin is P_0, and the θ_x-axis is in the direction of the proper motion of P relative to S. Then the position of the star in these coordinates is expressed as

$$(\theta_x, \theta_y) = (\mu t_0, \mu t_d) . \quad (7)$$

This maps two of the parameters of the residual function, t_0 and t_d, to a point on the celestial sphere. When the relative position of a star on the celestial sphere is (1)–(6) of Figure 6, the residual curve becames like curve (1)–(6) of Figure 5, respectively.

Once the coefficients c_j in equation (6) are fixed, it is easy to evaluate the maximum residual $R_{\rm Max}$. Since c_j are the function of the above coordinates of the star, we can illustrate $R_{\rm Max}$ as a function of the coordinates as in Figure 7, where we obtained $R_{\rm Max}$ for the ranges $0 \le \theta_x \le 4.5\mu T$ and $0 \le \theta_y \le 4\mu T$ numerically. Note that the spacetime reversibility assures that $R_{\rm Max}$ is symmetric with respect to the θ_x- and θ_y-axes. The maximum residual becomes small when the third derivative of $f(t)$ happens to be small. This explains the six wedges of the projected contours in Figure 7. The time delay effect will be detectable when $R_{\rm Max}$ is larger than $R_{\rm crit}$, which is expressed by the uncertainty of the TOA observation $\sigma_{\rm TOA}$ and the mass of the star M_S as

$$R_{\rm crit} = \frac{\sigma_{\rm TOA}}{(M_S/M_\odot) \times 9.851\ \mu{\rm s}} . \quad (8)$$

Once R_{crit} is given, the region of the stars that will cause the detectable delay is fixed. This region is illustrated in Figure 8. The area of this region A_D is proportional to $(\mu T D_S)^2$, where D_S is the distance of the star from the observer and its coefficient C_D is the function of R_{crit} as

$$A_D = C_D(R_{crit})(\mu T D_S)^2 . \quad (9)$$

Here the subscript D stands for "detectable." Rough estimations of the coefficient are numerically obtained as $C_D(0.01) \approx 15$, $C_D(0.1) \approx 4$ and $C_D(0.2) \approx 2.5$.

On the other hand, in order to measure the three parameters with sufficient precisions, we should impose a tighter condition. First, we note that in order to determine t_0, we should detect the quartic trend in the residual. For the stars on the θ_x-axis, the quartic trend is detectable when $|\theta_y| < 1.2\mu T$ in the case $R_{crit} = 0.01$ and when $|\theta_y| < 0.6\mu T$ in the case $R_{crit} = 0.1$. Next, after t_0 is fixed, we simplify the process to determine the remaining two parameters, t_d and M_S, by removing a part of the observational data so as to make the reduced period of observation symmetric with t_0. Then the estimation process reduces to a fitting by an even function. Since we estimate the quadratic trend simultaneously, the reduced observation period should be long enough so that the deviation of the characteristic function from a quadratic function of time is significant. This is roughly equivalent to the condition that the original observation period covers both of the inflection points of the characteristic function so that the function cannot be expanded by a low-degree polynomial within this period, namely, $|t_0| + |t_d| < T/2$. Thus the condition becomes that the gravitating star should locate within the square region composed by the points where (θ_x, θ_y) are $(\pm 0.5\mu T, 0)$ or $(0, \pm 0.5\mu T)$. The resulting area becomes

$$A_M = C_M(R_{crit})(\mu T D_S)^2 , \quad (10)$$

where the subscript M stands for "measurable." Here C_M asymptotes to 0.5 when M_S is large enough for detecting a quartic trend at $\theta_y = 0.5\mu T$, that is, when $R_{crit} < 0.3$. On the contrary, when $R_{crit} > 0.3$, namely when $M_S < 0.07\ M_\odot$ in the case $\sigma_{TOA} = 200$ ns, $C_M(R_{crit})$ is smaller than 0.5.

Now, note that

$$\mu T D_S = |\mu_P - \mu_S| T D_S = \left| \frac{D_S}{D_P} V_P - V_S \right| T , \quad (11)$$

where μ_P and μ_S are the proper motion vectors of the pulsar and the star, V_P and V_S are the transverse velocity vectors of the pulsar and the star. Then, if we fix the pulsar and the observation period, the areas depend only on R_{crit}, D_S, and V_S.

If the distribution of the mass, the position, and the velocity of foreground stars are known, we can estimate the probability to detect (or measure) such time delay effect by the foreground stars during the period T by integrating A_D (or A_M) with respect to the mass, the position, and velocity. Note that the dependency with D_S and V_S is the same for both of A_D and A_M. The difference between these two areas only comes from the dependency on R_{crit}.

Here we will consider only a rough estimation under simplified assumptions shown below. On the mass distribution, we assume that all stars have the same mass M_S. As for the positional distribution, we adopt a single-component exponential disk with the scale height h and the total column density Σ_S. According to the recent study, the velocity of the pulsar can be expected to be much larger than that of the stars (Lyne & Lorimer 1994). So we assume $V_S \approx 0$ for all stars. In this case,

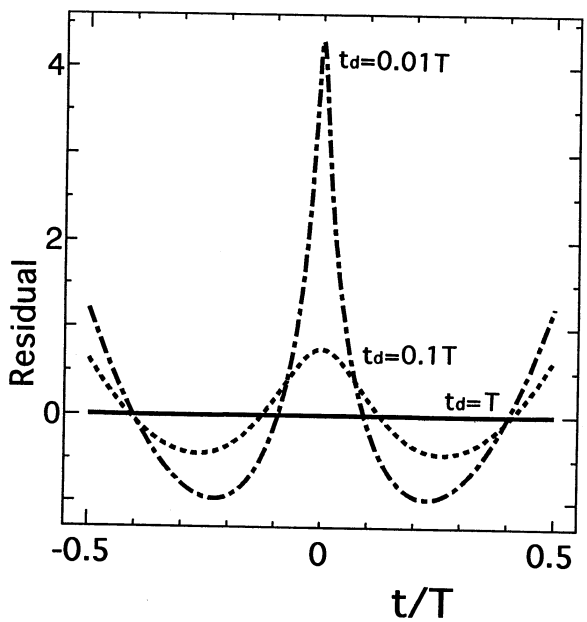

FIG. 4a

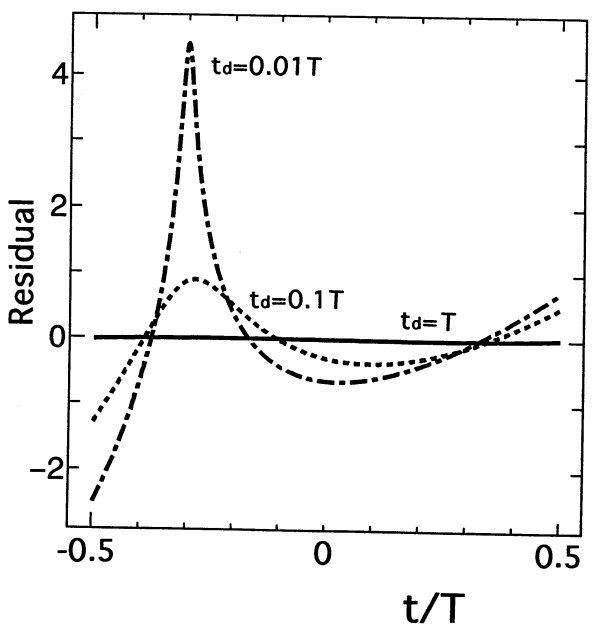

FIG. 4b

FIG. 4.—Amplitude of the residuals for various t_d/T. The residuals for the cases (*a*) $t_0 = 0T$ and (*b*) $t_0 = -0.3T$. The dash-dotted line is for the case $t_d = 0.01T$, the dashed line is for the case $t_d = 0.1T$, and the solid line is for the case $t_d = T$. Although the time variation of the residuals is not significant for the case $t_d = T$ in this scale, it has the same properties with respect to time which are clearly shown in Fig. 5*b*. The smaller is t_d/T, the larger becomes the height of the hump of residuals at the epoch t_0.

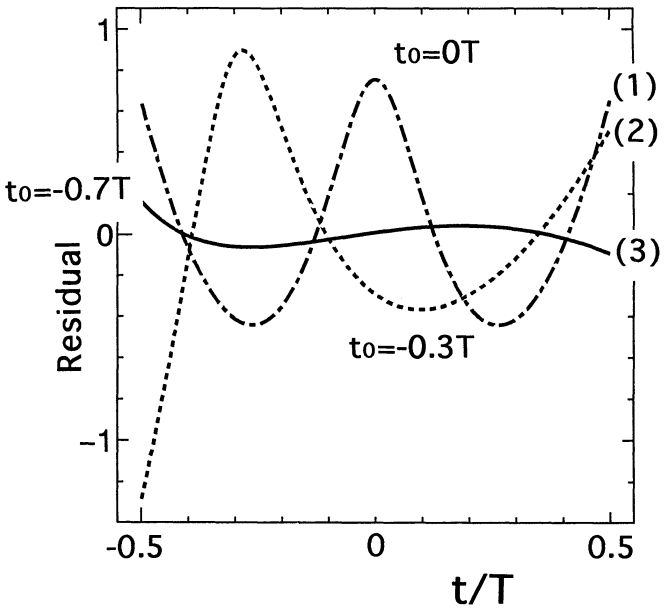

FIG. 5a

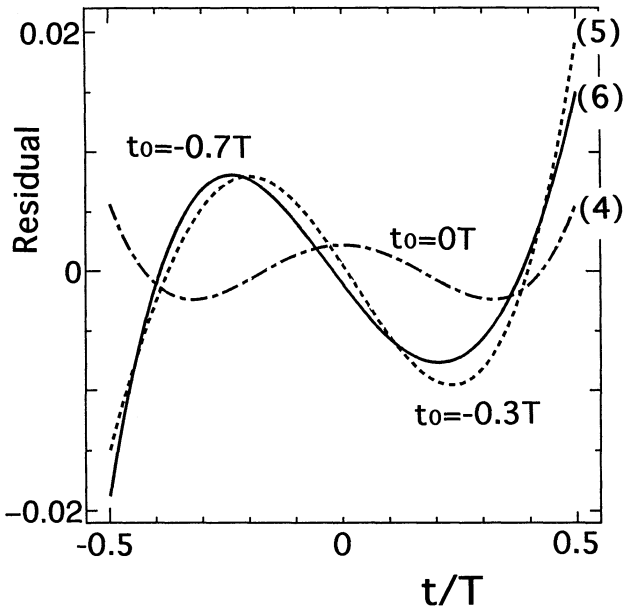

FIG. 5b

FIG. 5.—Shape of the residuals for various t_0/T. The residuals for the cases (*a*) $t_d = 0.1T$ and (*b*) $t_d = T$. The dash-dotted line (1), (4) is for the case $t_0 = 0T$; the dashed line (2), (5), the case $t_0 = -0.3T$; and the solid line (3), (6), the case $t_0 = -0.7T$. When t_d/T is larger, the relative width of the hump of residuals becomes somewhat wider and the height of the hump becomes smaller. Note that the observation period T is less than a few decades at most. Hence (*b*) will be a typical case in practical observation to detect this effect.

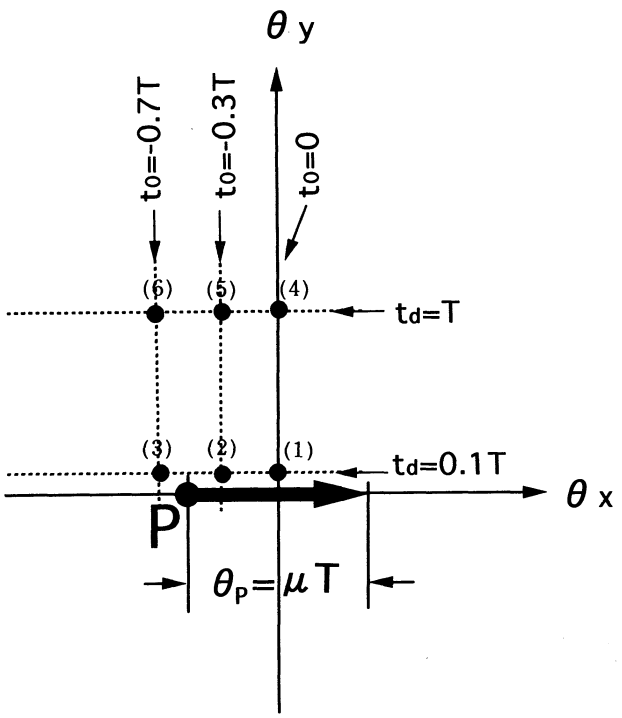

FIG. 6.—Relations in apparent positions of the pulsar and the star for six cases of Fig. 5. The origin was taken as the position of the pulsar when $t = 0$. The position of the pulsar becomes $(\theta_x, \theta_y) = (\mu t, 0)$. The point $(t_0/T, t_d/T)$ in the parameter space relates to the position of the star $(\mu t_0, \mu t_d)$ in this coordinate system. The six cases (1)–(6) of Fig. 5 correspond to the relative positions of the star (1)–(6) as indicated.

the shape of the integration region becomes conelike. Then the probability of detectable event during the observation period Γ is expressed as

$$\Gamma_{(D,M)} = C_{(D,M)}(R_{crit})(V_P T)^2\left(\frac{\Sigma_S}{2M_S h}\right)\left(\frac{D_P}{3}\right)K\left(\frac{D_P \sin|b_P|}{h}\right), \tag{12}$$

where b_P is the galactic latitude of the pulsar and

$$K(x) \equiv \int_0^x \xi^2 e^{-\xi}\,d\xi \Big/ \int_0^x \xi^2\,d\xi = 3x^{-3}[2 - (x^2 + 2x + 2)e^{-x}] \tag{13}$$

is the latitude-dependency coefficient, which is illustrated in Figure 9. Note that $K(x) \approx 2^{-x}$ when $0 \le x < 2$, $K(x) \approx x^{-2}$ when $2 \le x < 6$, and $K(x) \approx 6x^{-3}$ when $6 \le x$.

Now let us assume $\sigma_{TOA} = 200$ ns, $T = 10$ yr, $V_P = 400$ km s^{-1}, $D_P = 2$ kpc, $M_S = 0.2\,M_\odot$, which is the value of typical M dwarfs, $h = 325$ pc (Bahcall 1986), and $\Sigma_S = 40\,M_\odot$ pc^{-2} (Bahcall 1984) as nominal values. Then $R_{crit} = 0.1$ and the probability is evaluated as

$$\Gamma_{(D,M)} \approx \left(\frac{1}{75}, \frac{1}{600}\right)\left(\frac{D_P}{2\text{ kpc}}\right)\left(\frac{V_P}{400\text{ km s}^{-1}}\right)^2\left(\frac{T}{10\text{ yr}}\right)^2 \times \left(\frac{\Sigma_S}{40\,M_\odot\text{ pc}^{-2}}\right)\left(\frac{h}{325\text{ pc}}\right)^{-1}\left(\frac{M_S}{0.2\,M_\odot}\right)^{-1} \times \exp\left[-4.27\sin|b_P|\left(\frac{D_P}{2\text{ kpc}}\right)\left(\frac{h}{325\text{ pc}}\right)^{-1}\right] \tag{14}$$

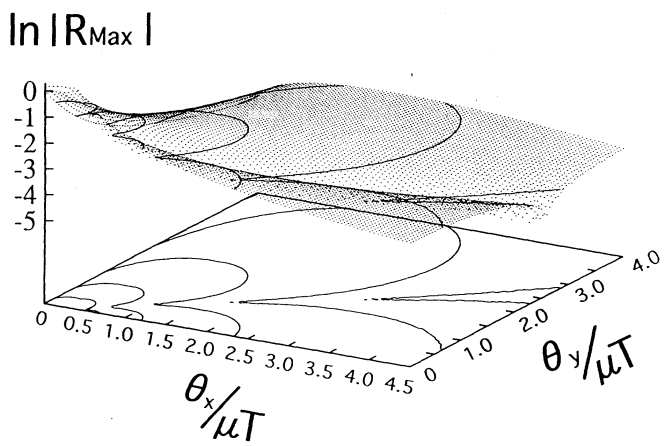

FIG. 7.—Maximum residual per unit mass as a function of the star's position relative to the pulsar. We assume that the pulsar shifts its position from $(-0.5\mu T, 0)$ to $(0.5\mu T, 0)$ during the observation period. The maximum residual per unit gravitating mass $R_{\rm Max}$ was obtained numerically as a function of the star's angular coordinates (θ_x, θ_y). The z-coordinate represents the $\log |R_{\rm Max}|$. Suppose that the time delay effect is detectable when $R_{\rm Max} > R_{\rm crit}$. Then, the detectable region of the stars is $\log R_{\rm Max} > -2$ when $R_{\rm crit} = 10^{-2}$, and $\log R_{\rm Max} > -1$ when $R_{\rm crit} = 10^{-1}$.

for low-latitude pulsars, say $|b_{\rm P}| < 20°$, and

$$\Gamma_{(\rm D,M)} \approx \left(\frac{1}{610}, \frac{1}{4900}\right)\left(\frac{D_{\rm P}}{2\ \rm kpc}\right)^{-1}\left(\frac{V_{\rm P}}{400\ \rm km\ s^{-1}}\right)^{2} \times \left(\frac{T}{10\ \rm yr}\right)^{2}\left(\frac{\sin|b_{\rm P}|}{0.5}\right)^{-2}\left(\frac{\Sigma_{\rm S}}{40\ M_\odot\ \rm pc^{-2}}\right) \times \left(\frac{h}{325\ \rm pc}\right)\left(\frac{M_{\rm S}}{0.2\ M_\odot}\right)^{-1}. \quad (15)$$

for high-latitude pulsar, say $|b_{\rm P}| > 20°$.

The number of known millisecond pulsars on the Galactic plane are more than a dozen (Taylor, Manchester, & Lyne 1993; Phinney & Kulkarni 1994). Since $\Gamma_{\rm D}$ is a few percent for low-latitude Galactic millisecond pulsars, the probability of detecting this effect might be small even if we observe all of these pulsars. However, the probabilities are proportional to T^2, and they become large as the TOA observation uncertainty decreases. Further, many new millisecond pulsars will be found as the observation sensitivity improves. In the future, it will be more probable to detect this effect.

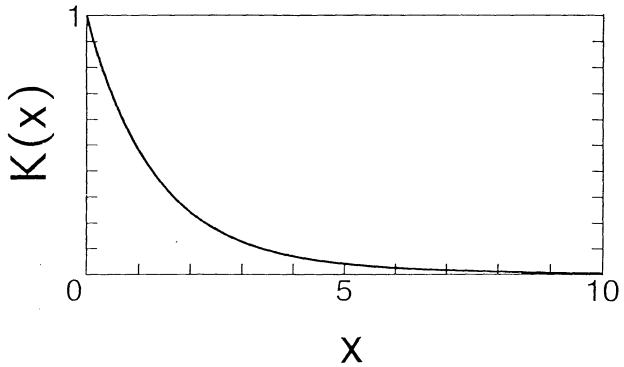

FIG. 9.—Latitude-dependency function. The figure illustrates a characteristic function, $K(x) = 3x^{-3}[2 - (x^2 + 2x + 2)e^{-x}]$, expressing the dependency with respect to the pulsar's latitude of the detectable (or measurable) probability of the gravitational time delay effect by a foreground star in pulsar timing observation.

Let us briefly discuss how to identify the star causing the delay. Assume that the position and the proper motion of the pulsar are obtained. Also assume that the star causing the delay is so bright that the star is visible and its proper motion relative to the pulsar is measurable. In this case, once the effect is detected and at least the parameter t_0 is determined, one constraint for the candidate stars is fixed. That is, the direction of the motion of the star relative to the pulsar should be

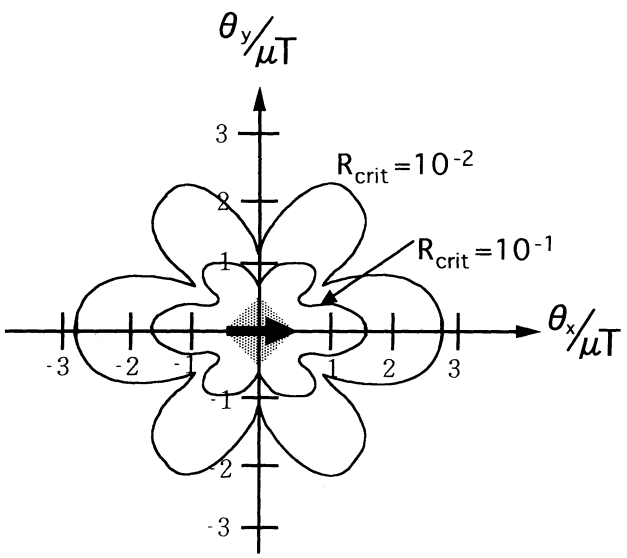

FIG. 8.—Detectable and measurable regions on a celestial sphere. The inside of rosette-like contours are the detectable regions corresponding to the indicated values of $R_{\rm crit}$. The shaded square is the measurable region, which is unchanged when $R_{\rm crit} < 0.3$. The thick arrow indicates the movement of the pulsar during the observation period.

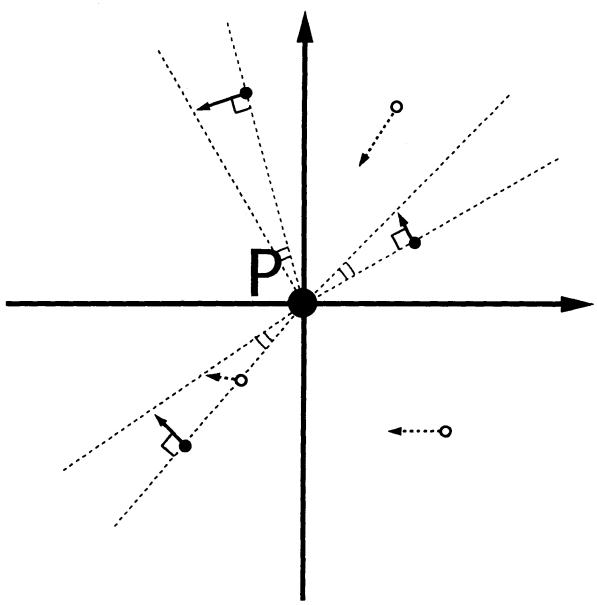

FIG. 10.—Star flow diagram. A pulsar-centered star atlas at t_0. Arrows indicate the proper motion of the stars relative to the pulsar. The filled circles are the candidate stars that have the appropriate ratio of θ_0 to μ, and have no radial component of the relative proper motion. Open circles denote non-candidate stars.

orthogonal to the arc connecting the pulsar and the star at the epoch t_0. This will be helpful in identifying the star causing the delay. If the candidate star is found by this constraint, the parameter t_d will be obtained by measuring the minimum separation θ_0 and the relative proper motion μ. Then the mass of the star, the last parameter of this time delay, will be determined from the amplitude of the residual. Namely, there is a possibility of obtaining the mass of the star by combining with the optical observation even the star is out of the "measurable" region.

In the case that all three parameters are determined by TOA data analysis only, it will be easier to identify the star. Because of one more constraint, the information on t_d, can be used for the identification. Consider a "star flow diagram," a pulsar-centered star atlas when the proper motions of all stars relative to the pulsar at the epoch t_0 are indicated by arrows, as shown in Figure 10. Then, the candidates will be the stars in the diagram whose ratio of the separation angle to the proper motion is equal to t_d and which have no radial component of the relative proper motion. In Figure 10, filled and open circles denote the candidates and noncandidate stars, respectively. On the other hand, if there are no visible candidate stars, the time delay might be caused by a MACHO.

4. DISCUSSION

So far we have assumed that there is no other effect that causes the cubic and the higher trends in the residual. Under that condition, we have seen that in most cases, except the case when t_d is less than the length of the observation period and t_0 is near the center of the observation period, the residuals of the time delay effect caused by the foreground star appear as a cubic trend after a quadratic polynomial is fitted. Table 2 shows the estimated parameters for some known pulsars. The breaking index, $n \equiv (\nu\ddot{\nu})/\dot{\nu}^2$, is proved to be 3 when the cubic trend is due to the magnetic dipole radiation.

For some pulsars, cubic trends have been observed to be much larger than expected from the radiation theory (Thorsett, Arzoumanian, & Taylor 1993; Backer, Foster, & Sallmen 1993; Kaspi, Taylor, & Ryba 1994). In such cases, it might be worth reanalyzing the TOA data by introducing this effect. It should be noted that, as shown in Table 1, there are many causes of the cubic trend. So it seems to be difficult to separate the time delay effect discussed here from these other effects. This is true if the TOA analysis is done only for one data set. Note that the magnitude of the residual for this effect will change according to the length of the observation period. Therefore, when the observation is continued and the enlarged data are reanalyzed for a longer observation period, we will be able to judge whether the trend is caused by this effect or not. To compare this effect with others and to evaluate the separability quantitatively remain an open question.

Let us consider the application of the TOA analysis in estimating the mass of MACHOs. Recently some MACHO candidates were discovered by the microlensing events and their masses were estimated to be of the order of 0.1 $M_\odot$ (Aubourg et al. 1993; Alcock et al. 1993). However, these estimates were obtained under many assumptions. The mass of a MACHO is important in specifying what kind of object the MACHO is. In the determination of the mass of MACHOs, the method proposed in this paper may have some theoretical advantages. That is, no assumption is made on the proper motion and the distance of MACHOs and the pulsars. In fact, we need not know the position of MACHOs.

As for the velocities of MACHOs, their mean value is thought to be ~ 200 km s^{-1}, which is much larger than that of the random motion of nearby stars. Therefore, in calculating the probability to detect the effect caused by MACHOs, the approximation $V_S \ll V_P$ adopted in § 3 is not appropriate. In the case where V_S and V_P are the same order of magnitude and the distribution of V_S is random, there appears an additional term in the expression of $\Gamma_{(D,M)}$, which is based on the integration of $(V_S T)^2$ term in a column-like region along the pulsar's direction.

By taking this contribution into consideration also, we may roughly estimate the probability for the case of MACHOs. Let us assume that the distribution of MACHOs is uniform and isotropic, whose density is $\rho \approx 7.9 \times 10^{-3}\ M_\odot/(\mathrm{pc})^3$. Further assume that $M_S = 0.1\ M_\odot$ and $V_S = 200$ km s^{-1}, and use the same values for the other parameters. Then

$$\Gamma_{(D,M)} \approx \left(\frac{1}{290}, \frac{1}{1300}\right)\left(\frac{D_P}{2\ \mathrm{kpc}}\right)\left(\frac{T}{10\ \mathrm{yr}}\right)^2 \times \left(\frac{\rho}{7.9 \times 10^{-3}\ M_\odot\ \mathrm{pc}^{-3}}\right)\left(\frac{M_S}{0.1\ M_\odot}\right)^{-1} \times \left[\frac{4}{7}\left(\frac{V_P}{400\ \mathrm{km\ s^{-1}}}\right)^2 + \frac{3}{7}\left(\frac{V_S}{200\ \mathrm{km\ s^{-1}}}\right)^2\right]. \quad (16)$$

These are roughly the half of the values of Γ by the stars for a pulsar on Galactic plane and are 3 times larger than those for

TABLE 2

FREQUENCY CHARACTERISTICS OF SOME PULSARS

PSR	P (s)	$\dot{P}$ (10^{-15})	$\ddot{\nu}$ (10^{-21} s^{-3})	n
B0531+21[a]	0.033	420.9	9.76 ± 0.07	2.05 ± 0.01
B0540−69	0.050	479.1	3.66 ± 0.04	2.04 ± 0.02
B1509−58	0.150	1540	1.96 ± 0.01	2.80 ± 0.01
B1620−26[b]	0.011	81.56E−5	(1.866 ± 0.017)E−2	(3.812 ± 0.035)E+7
B1757−24	0.125	127.9	(3.2 ± 0.4)E−1	38 ± 5
B1937+21[c]	1.56E−3	1051E−7	(13.2 ± 0.3)E−6	(4.52 ± 0.10)E+3
B2127+11A[d]	0.11	−0.02	(4.8 ± 0.1)E−4	1.5E+6

[a] Crab Pulsar.
[b] In M4.
[c] Fastest millisecond pulsar.
[d] In M15.

NOTES.—P is the period of pulse, $\dot{P}$ is the period derivative, $\ddot{\nu}$ is the second-order derivative of the pulse frequency, and n is the braking index. These data are quoted from Taylor, Manchester, & Lyne 1993 and Kaspi, Taylor, & Ryba 1994.

high-latitude case. For more rigorous evaluation, we need a more realistic distribution function with respect to the mass, the position, and the velocity of MACHOs.

In summary, we introduced a new correction term to the model of TOA data analysis, i.e., the gravitational time delay caused by a foreground star. The effect appears in the form of $\log(1 + t^2)$, whose amplitude is directly connected to the mass of the star. We discussed the practical aspects of the mass measurement of the star by detecting this term. It is worth noting that the explicit information on the distances to the star and/or to the pulsar is not necessary. We illustrated the characteristics of this effect and how to separate the time variation due to this effect from other effects. When the residual of the TOA has a positive hump and its time-dependency agrees with the tendency expected from this effect, it is worth reanalyzing the TOA data by introducing three new parameters; the mass of the foreground star, the epoch of the closest approach, and the proper motion of the star relative to the pulsar. Such fitting will determine the mass of the star. Since a vast amount of TOA data has already been accumulated for a number of pulsars, it is desirable to detect this effect.

We would like to thank N. Arimoto, O. Doroshenko, T. Ebisuzaki, M. Fujishita, Y. Hanado, M. Imae, T. Ishida, T. Kamae, S. Kopeikin, M. Miyamoto, and M. Sekido for their helpful comments. We thank A. Gould for his valuable suggestions and comments. This work was partly supported by the Japanese Science and Technology Agency Fellowship (K. O.) and the NAO Joint Research Fund.

APPENDIX A

APPROXIMATION OF GRAVITATIONAL TIME DELAY FORMULA

In this appendix, we will examine the conditions necessary to find an approximation for the gravitational time delay, as in equation (1).

Denote the distance between S and the line OP by L (see Fig. 1). If we introduce the auxiliary quantities x, y, z defined as

$$x \equiv \tan\frac{\theta}{2}, \qquad y \equiv \frac{\mathrm{OS}}{\mathrm{SP}}, \qquad z \equiv \left(\frac{L}{\mathrm{SP}}\right)^2 = \left(\frac{2xy}{1+x^2}\right)^2, \tag{17}$$

then the amount of gravitational time delay is expressed as

$$\begin{aligned}\Delta t &= (1+\gamma)\frac{GM}{c^3}\ln\left|\frac{\mathrm{OS}+\mathrm{SP}+\mathrm{OP}}{\mathrm{OS}+\mathrm{SP}-\mathrm{OP}}\right| \\ &= -(1+\gamma)\frac{GM}{c^3}\left(\ln\left|\tan\frac{\mathrm{OS}}{2}\right| + \ln\left|\tan\frac{\angle\mathrm{POS}}{2}\right|\right) \\ &= -(1+\gamma)\frac{GM}{c^3}f(x, y)\,,\end{aligned} \tag{18}$$

where

$$f(x, y) \equiv 2\ln|x| + \ln|y| - \ln|1+x^2| - \ln\left|\frac{1+\sqrt{1-z}}{2}\right|. \tag{19}$$

Note that $0 \le z \le 1$ by definition.

In approximating $f(x, y)$, we assume that θ is small as of the order of 1″. Under this condition, $x \sim \theta/2 \ll 1$ and $z \sim (2xy)^2$. Then the first term, $2\ln|x|$, becomes the main part of $f(x, y)$ unless $z \sim 1$. The condition $x \ll 1$ means that the angle $\angle$OPS is small and $\angle\mathrm{OPS} \sim 2xy$, while the fact $z \sim 1$ means that the angle $\angle$OPS is large and the star is quite close to the pulsar. In the latter case,

$$f(x, y) \approx 2\ln|x| + \ln|y| - (\ln|x| + \ln|y|) = \ln|x|\,. \tag{20}$$

However, in general this case may be rare. Also the coefficient of the main term changes by the factor $\frac{1}{2}$ at most. Thus, hereafter, we will consider only the case $z \ll 1$. Namely, we assume that the star is not so close to the pulsar or the observer, say at a distance of 1 pc or larger from both the pulsar and the observer.

Let us examine the magnitude of the maximum variations of the other three terms of $f(x, y)$ caused by the proper motion of the star and the pulsar. Here, we assume the duration of the observation as 10 yr and the uncertainty of TOA as 200 ns, and we will consider the star with $0.2\,M_\odot$. Since the factor $(1+\gamma)GM_\odot/c^3$ is $\sim 10\,\mu$s, we may neglect terms in $f(x, y)$ if their variation is less than 0.1 for 10 yr.

First, the variation of the second term is evaluated as

$$\Delta\ln|y| \le \frac{|\Delta\mathrm{OS}|}{\mathrm{OS}} + \frac{|\Delta\mathrm{SP}|}{\mathrm{SP}} < \frac{2|\Delta\mathrm{OS}|}{\mathrm{Min}\,(\mathrm{OS}, \mathrm{SP})} + \frac{|\Delta\mathrm{OP}|}{\mathrm{SP}}. \tag{21}$$

Note that the velocities of the star and the pulsar can be as large as 100 and 800 km s^{-1}, respectively. Then, the maximum of ΔOS and ΔOP during a period of 10 yr will amount to 200 and 1600 AU, respectively. If we substitute these values into the above

inequality, the maximum variation of this term is evaluated to be less than 8×10^{-3} when Min (OS, SP) > 1 pc, and therefore, is negligible.

Next, the variation of the third term is caused by the transverse component of the motions of the star relative to the pulsar as

$$-\Delta \ln |1 + x^2| \approx -2x \Delta x \approx -\frac{1}{2}\left(\frac{L}{\mathrm{OS}}\right)\left(\frac{\Delta L}{\mathrm{OS}}\right), \tag{22}$$

where we used the assumption $x \ll 1$. Then, even if we substitute the maximum of ΔL, i.e., 1600 AU, the variation of his term is less than the order of 10^{-2}, and therefore, is negligible.

Finally, the variation of the fourth term becomes

$$-\Delta \ln \left|\frac{1 + \sqrt{1 - z}}{2}\right| \approx \frac{\Delta z}{4} \approx \frac{z}{2}\left(\Delta \ln |x| + \Delta \ln |y|\right), \tag{23}$$

where we used $x \ll 1$ again. Since $z < 1$ and $\Delta \ln |y|$ is negligible as we have seen in the above, $z \Delta \ln |y|$ is small enough to be ignored. On the other hand,

$$\frac{z}{2} \Delta \ln |x| \approx 2(xy^2)(\Delta x) \approx \frac{1}{2}\frac{L}{\mathrm{OS}}\left(\frac{\mathrm{OS}}{\mathrm{SP}}\right)^2 \frac{\Delta L}{\mathrm{OS}} < \frac{\Delta L}{\mathrm{SP}}. \tag{24}$$

If the maximum of ΔL is substituted in, the maximum variation of this term is less than 10^{-2}, and therefore is negligible.

On the contrary, the variation of the first term of $f(x, y)$ is mainly due to the transverse component of the relative motion. Thus it should be examined carefully. The variation in this term is expressed as

$$\Delta \ln |x| \approx \frac{\Delta x}{x} \approx \frac{\Delta \theta}{\theta} = \frac{\Delta L}{L}. \tag{25}$$

Note that we assume that θ is so small that we can approximate $x = \tan(\theta/2) \approx \theta/2$. Let us take the value of L as 500 AU (i.e., $\theta = 1''$ at OS = 500 pc) and that of the transverse component of the relative velocity as 30 km s^{-1} as a realistic case. Then ΔL amounts to 60 AU during 10 yr. In this case, the variation of the first term amount to 0.12. In other words, the variation of Δt arising from this term is 240 ns for the star whose mass is 0.2 $M_\odot$.

Therefore we only have to consider this term in $f(x, y)$, and we can approximate as

$$f(x, y) \approx \ln\left(\frac{\theta}{2}\right)^2. \tag{26}$$

Now, under the same conditions, the time variation of the separation angle θ is approximated as

$$\theta(t) = \sqrt{\theta_0^2 + \mu^2(t - t_0)^2} = \theta_0 \sqrt{1 + \left(\frac{t - t_0}{t_d}\right)^2}. \tag{27}$$

By substituting this into equation (26), we obtain equation (1).

APPENDIX B

EXPECTED RESIDUAL CURVE $R(t)$

As an example, let us show how to evaluate the residual curve for the foreground star of a unit mass $R(t)$, which would be expected after the least-square fitting of a quadratic polynomial. Here we take t, t_0, and t_d are scaled by the observation period T, i.e., $\tau = t/T$, $\tau_0 = t_0/T$, and $\tau_d = t_d/T$. Then, the residual is defined as

$$R(\tau) \equiv f(\tau) - P(\tau), \tag{28}$$

where

$$P(\tau) = \sum_{j=0}^{2} c_j \tau^j \tag{29}$$

is the best-fit polynomial for the characteristic function

$$f(\tau) = -\ln\left[1 + \left(\frac{\tau - \tau_0}{\tau_d}\right)^2\right] \tag{30}$$

in the interval $(-\frac{1}{2}, \frac{1}{2})$. The coefficients c_j are determined by solving the normal equation

$$\begin{pmatrix} I_0 & I_1 & I_2 \\ I_1 & I_2 & I_3 \\ I_2 & I_3 & I_4 \end{pmatrix}\begin{pmatrix} c_0 \\ c_1 \\ c_2 \end{pmatrix} = \begin{pmatrix} J_0 \\ J_1 \\ J_2 \end{pmatrix}. \tag{31}$$

Let us assume the observation of TOAs are sufficiently homogeneous and dense through the entire period of observation. Then the coefficients of the normal equation are approximated as $I_n = 0$ for odd n,

$$I_n = \int_{-1/2}^{1/2} \tau^n d\tau = \frac{1}{(n+1)2^n} \tag{32}$$

for even n, and

$$J_n = -\int_{-1/2}^{1/2} \tau^n \ln\left[1 + \left(\frac{\tau - \tau_0}{\tau_d}\right)^2\right] d\tau \,. \tag{33}$$

By substituting equations (32) and (33) into equation (31) and deriving the inverse matrix, we solved the coefficients c_j in terms of J_n as

$$\begin{pmatrix} c_0 \\ c_1 \\ c_2 \end{pmatrix} = \begin{pmatrix} 9/4 & 0 & -15 \\ 0 & 12 & 0 \\ -15 & 0 & 180 \end{pmatrix} \begin{pmatrix} J_0 \\ J_1 \\ J_2 \end{pmatrix} . \tag{34}$$

The integrals J_n are evaluated analytically as

$$J_0 = -\tau_d K_0 \,, \tag{35}$$

$$J_1 = -\tau_d^2 K_1 - \tau_0 \tau_d K_0 \,, \tag{36}$$

$$J_2 = -\tau_d^3 K_2 - \tau_0 \tau_d^2 K_1 - \tau_0^2 \tau_d K_0 \,, \tag{37}$$

where

$$K_0 = \{\tau[\ln(1+\tau^2) - 2] + 2\tan^{-1}\tau\}_a^b \,, \tag{38}$$

$$K_1 = \left\{\frac{\tau^2}{2}[\ln(1+\tau^2) - 1] + \frac{1}{2}\ln(1+\tau^2)\right\}_a^b \,, \tag{39}$$

$$K_2 = \left\{\frac{\tau^3}{3}\left[\ln(1+\tau^2) - \frac{2}{3}\right] + \frac{2}{3}(\tau - \tan^{-1}\tau)\right\}_a^b \,, \tag{40}$$

and

$$a = -\frac{1 + 2\tau_0}{2\tau_d} \,, \qquad b = \frac{1 - 2\tau_0}{2\tau_d} \,. \tag{41}$$

By combining the above expressions, we can obtain expressions for $P(\tau)$ and $R(\tau)$.

REFERENCES

Alcock, C., et al. 1993, Nature, 365, 621
Aubourog, E., et al. 1993, Nature, 365, 623
Backer, D. C., Foster, R. S., & Sallmen, S. 1993, Nature, 365, 817
Backer, D. C., & Hellings, R. W. 1986, ARA&A, 24, 537
Bahcall, J. R. 1984, ApJ, 276, 169
———. 1986, ARA&A, 24, 591
Hosokawa, M., Ohnishi, K., Fukushima, T., & Takeuti, M. 1993, A&A, 278, L27
Kaspi, V. M., Taylor, J. H., & Ryba, M. F. 1994, ApJ, 428, 713
Lyne, A. G., & Lorimer, D. R. 1994, Nature, 369, 127
Manchester, R. N., & Taylor, J. H. 1977, Pulsars (San Francisco: Freeman)
Paczyński, B. 1986, ApJ, 304, 1
Phinney, E. S., & Kulkani, S. R. 1994, ARA&R, 32, 591
Ryba, M. F., & Taylor, J. H. 1991, ApJ, 371, 739
Shapiro, I. 1964, Phys. Rev. Lett., 13, 789
Taylor, J. H., & Weisberg, J. M. 1989, ApJ, 345, 434
Taylor, J. H., Manchester, R. N., & Lyne, A. G. 1993, ApJS, 88, 529
Thorsett, S. E., Arzoumanian, Z., & Taylor, J. H. 1993, ApJ, 412, L33
Udalski, A., et al. 1993, Acta Astron., 43, 289

Note added in proof.—After this paper was submitted for publication, we were aware of the work by T. I. Larchenkova & O. V Doroshenko (A&A, in press [1995]), which gives a discussion similar to what we presented in § 2.